CRREL Report 82-3

February 1982

Breakup of solid ice covers due to rapid water level variations

Lennart Billfalk

Prepared for
OFFICE OF THE CHIEF OF ENGINEERS

REPORT DOCUMENTATION PAGE

READ INSTRUCTIONS BEFORE COMPLETING FORM

1. REPORT NUMBER: CRREL Report 82-3
2. GOVT ACCESSION NO.:
3. RECIPIENT'S CATALOG NUMBER:

4. TITLE (and Subtitle): BREAKUP OF SOLID ICE COVERS DUE TO RAPID WATER LEVEL VARIATIONS
5. TYPE OF REPORT & PERIOD COVERED:
6. PERFORMING ORG. REPORT NUMBER:

7. AUTHOR(s): Lennart Billfalk
8. CONTRACT OR GRANT NUMBER(s): DACA 89-81-M-1536

9. PERFORMING ORGANIZATION NAME AND ADDRESS: Swedish State Power Board
10. PROGRAM ELEMENT, PROJECT, TASK AREA & WORK UNIT NUMBERS: CWIS 31353

11. CONTROLLING OFFICE NAME AND ADDRESS: Office of the Chief of Engineers, Washington, D.C. 20314
12. REPORT DATE: February 1982
13. NUMBER OF PAGES: 24

14. MONITORING AGENCY NAME & ADDRESS (if different from Controlling Office): U.S. Army Cold Regions Research and Engineering Laboratory, Hanover, New Hampshire 03755
15. SECURITY CLASS. (of this report): Unclassified
15a. DECLASSIFICATION/DOWNGRADING SCHEDULE:

16. DISTRIBUTION STATEMENT (of this Report)

Approved for public release; distribution unlimited.

17. DISTRIBUTION STATEMENT (of the abstract entered in Block 20, if different from Report)

18. SUPPLEMENTARY NOTES

19. KEY WORDS (Continue on reverse side if necessary and identify by block number)

Ice
Ice breakup
Ice formation
Rivers

20. ABSTRACT (Continue on reverse side if necessary and identify by block number)

The conditions that lead to initial breakup of a solid ice cover on a river due to rapid water level variations are analyzed. The analysis is based on the theory of beams on an elastic foundation. First cracking is assumed to occur when the bending moment induced in the ice cover by the wave exceeds the flexural strength of the ice cover.

PREFACE

This report was prepared by Lennart Billfalk, a hydraulic engineer of the Swedish State Power Board. The work was initiated at the Hydraulics Laboratory of the Power Board in Älvkarleby, Sweden. The study was supported by the Office of the Chief of Engineers (CWIS 31353, *Ice Effects on Energy Production*) and by the Power Board.

The author wishes to express appreciation to Dr. George D. Ashton, Dr. Krister Cederwall, Dr. Peter Larsen, and Dr. Devinder S. Sodhi for their valuable comments and reviews of the report. He also thanks Dr. Ashton and Guenther E. Frankenstein for the opportunity to stay at CRREL for one month to complete the work.

CONTENTS

ILLUSTRATIONS

TABLES

SYMBOLS

E	elastic modulus of ice
H	water depth
I	moment of inertia ($=d^3/12$ for a beam of unit width)
L	length of ice floe
M_x	bending moment at location x
M_0	end conditioning moment
P_0	end conditioning force
c	celerity of a surge wave
c_1, c_2, c_3, c_4	constants
d	thickness of ice cover
g	acceleration due to gravity
$\triangle h$	height of surge wave
$\triangle h_{crit}$	change in water level required to create shore cracks
k	modulus of the foundation ($=\rho g \approx 10^4$ N/m^2 for water)
ℓ	length of surge wave
ℓ_{cr}	length of surge wave that creates cracking of the ice cover
q	distributed load $= \triangle h \cdot k$
s	distance from the end of the surge wave to the ice cover edge
x, x', x''	length coordinates (defined in Fig. 4)
y	deflection of the ice
$1/\lambda$	characteristic length ($\lambda = [k/4EI]^{1/4}$)
σ_f	flexural strength of ice
ρ	density of water

BREAKUP OF SOLID ICE COVERS DUE TO RAPID WATER LEVEL VARIATIONS

Lennart Billfalk

INTRODUCTION

Purpose of the study

It is well known that rapid ice cover formation often reduces ice problems encountered at hydroelectric power plants. It is therefore common practice at many power stations to reduce the discharge and keep it as constant as possible during the beginning of freeze-up in order to facilitate the formation of a stable ice cover[6]. From experience, the operational staff usually gets some feeling for when and how flow regulation can start again without breaking the solid ice cover once it has formed. This problem is quite site-dependent, and very little theoretical or experimental work, on a more fundamental basis, has been done on the stability of solid ice covers[1,17].

One way to get direct information about what flow and water level variations an ice cover can withstand, on a specific river stretch, is to conduct a field test. Such tests have been undertaken by some power companies[10,11]. However, when analyzing observations from such field tests one finds it difficult to draw general conclusions regarding the mechanisms involved in the breakup of solid ice covers.

One "driving force" contributing to the breakup of solid ice covers is certainly the frictional forces on the ice, induced by increased flow velocities. Rapid discharge variations also cause surge waves that deform the ice cover. The purpose of the present study is to analyze under what circumstances rapid water level fluctuations can cause breakup (fracturing) of a solid river ice cover.

Stating the problem

Donchenko studied the conditions for ice jam formation in the tailwaters of hydroelectric power stations. He claimed that the dynamic destruction of the edge of the ice cover starts with the formation of cracks along the shores. After shore cracks have formed, debacles and hummocks form, and finally separation of the edge takes place[9].

The formation of shore cracks due to water level variations has also been studied by Billfalk, using the theory for beams on an elastic foundation[5]. The changes in water level ($\triangle h_{crit}$) required to create cracks along the river shores in an ice cover of thickness d, as found in that study, are

$$\triangle h_{crit} = 0.0058\ \sigma_f\ (d/E)^{1/2} \qquad (1)$$

assuming that the ice cover has a fixed end (frozen) along the shore. Assuming that the ice cover has a hinged end at the shore, cracks will occur at a distance $\pi/4\lambda$ out from the shoreline ($1/\lambda$ is a characteristic length defined later) if the variation of the water level exceeds

$$\triangle h_{crit} = 0.018\ \sigma_f\ (d/E)^{1/2} \qquad (2)$$

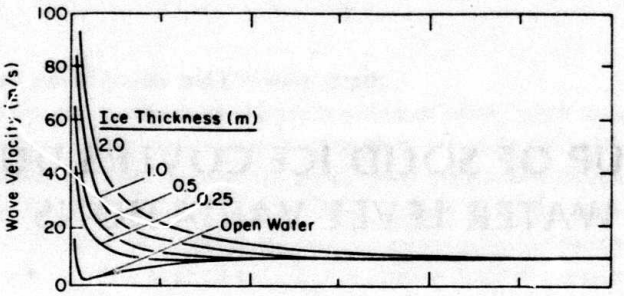

a. Phase velocity as a function of wave period.

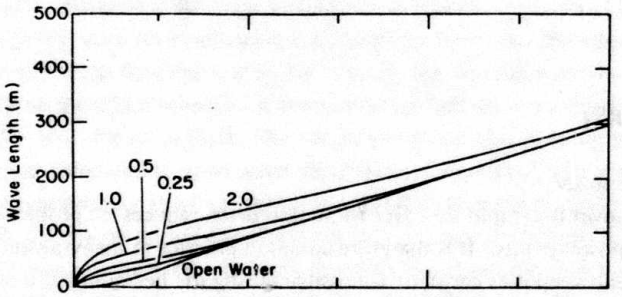

b. Wave length as a function of wave period.

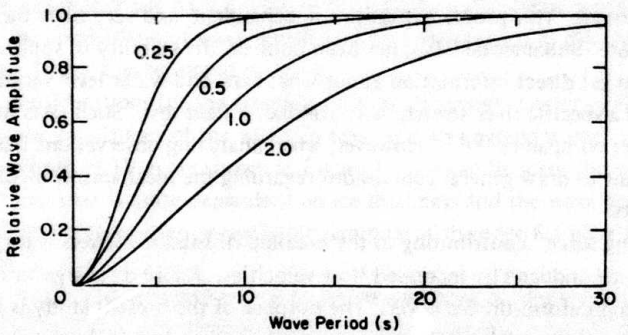

c. Damping of the amplitude as a function of wave period.

Figure 1. Modification of the characteristics of a sinusoidal wave passing under the edge of an ice cover (water depth 10 m). From Carter et al.[8].

where σ_f and E are the flexural strength and the elastic modulus of the ice, respectively. These expressions were derived using elastic theory, and they are not valid if the water level variation is slow. The elastic assumption is probably adequate if the critical water level fluctuation takes place within a minute[6].

Let us now consider a uniform prismatic channel upstream or downstream of a hydroelectric power station. An ice cover is assumed to exist on the channel and may extend to the powerhouse, or there may be open water for some distance away from the station.

Consider further a situation where the discharge is rapidly increased or decreased at the power station. For example, a linear increase of the flow with time will cause a nearly triangular-shaped negative wave to move upstream and a nearly triangular positive wave to move downstream from the station. At a decrease of the discharge, a positive wave travels away in the upstream direction and a negative wave in the downstream direction. The celerity c of such waves is approximately

$$c = (gH)^{1/2} \quad (3)$$

where g = acceleration of gravity and H = water depth.

If there is an ice cover on the water channel it will be deformed when the wave front passes. If the stresses in the ice sheet then exceed the strength of the ice, it will break.

Due to interaction between the wave and the ice cover the characteristics of the open water wave will be modified when it reaches the ice cover. Carter et al.[8] used a linearized wave theory to analyze the modification of the characteristics of a sinusoidal wave (wind wave) passing under the edge of an ice cover. The wave motion was described in terms of a velocity potential, both in the case of open water and of ice-covered water (the water depth strictly needs to be much larger than the ice thickness). By coupling the Bernoulli equation, which governs the wave motion, with the equation of motion for the ice plate under elastic bending, Carter et al. were able to show how the celerity of the wave on ice-covered water depends on the ice thickness and the wave period[8]. Their results regarding the celerity for a water depth of 10 m are shown in Figure 1a. As seen in this figure the phase velocity for short wave periods on ice-covered water is greatly increased, especially when the ice is thick. For longer periods the ice does not significantly modify the wave velocity as compared to open water conditions. Carter et al. also argued that the edge of the ice responds essentially at a frequency corresponding to the period of the incident wave, and concluded that the wave period therefore remains unchanged while the wave passes from the open water to the ice-covered water. In order to satisfy the condition that the wave length should equal the celerity of the wave times the wave period, it was found that the wave length must be modified as required by the phase velocity relation for ice-covered water. As can be seen from Figure 1a, this means that the lengths of short-period waves will increase when they enter the ice-covered water. The comparison of wave length for ice-covered water at different ice thicknesses is shown in Figure 1b for a water depth of 10 m.

Using energy considerations for the combined ice/water system, Carter et al. also derived a relation between the amplitudes of the waves in open and ice-covered water. Their results on this point for a water depth of 10 m are shown in Figure 1c. As can be seen, the damping of a wave passing under an ice cover is quite dependent on ice thickness and the wave period. However, for thin ice covers (0.25–0.50 m) there is negligible damping at the edge for wave periods larger than about 10 seconds.

What are the minimum wave lengths that might be generated by discharge variations at a hydroelectric power plant? Let us as an example assume that a rapid shutdown might take place in 5 to 10 seconds, and that the water depth in the channel is 5 m. From eq 1 it is seen that this would create a surge wave 35 to 70 m long. For a rough comparison with Carter's theory the surge wave might be considered as half a period (wave length) of a sinusoidal wave. The minimum "equivalent" wave period that should be considered when comparing waves generated by discharge changes in power stations with wind waves would, under these assumptions, be 10 to 20 seconds. For such wave periods the effect on the characteristics of a surge wave passing under an ice cover could probably be ignored in a first approximation, especially if the ice is thin.

It should be noticed that the characteristics of surge waves on rivers are affected by friction, and that the steepness and the height of the wave change along the channel (see, for example, Henderson[12]). Furthermore, very rapid discharge changes might create surges having a breaking front[12,18].

FRACTURING OF THE ICE COVER DUE TO THE PASSAGE OF SURGE WAVES

Basic assumptions

Consider the situation in Figure 2, where a triangular-shaped, positive or negative surge wave is reaching the edge of an ice cover. The stresses induced in the ice cover when the wave front

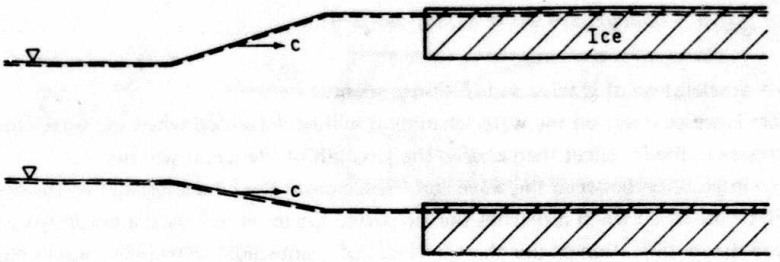

Figure 2. Negative and positive surge waves approaching the edge of an ice cover.

passes the edge will be estimated under the following simplifications and assumptions:

1. The deformation of the ice sheet due to the passage of a wave of the considered wave length takes place within 10 to 20 seconds. Even if some viscous deformation occurs during this time, brittle fracture of the ice will most probably occur[6]. Elastic deformation of the ice sheet is therefore assumed to give adequate results.
2. The channel is wide, or open cracks exist in the ice cover along the banks. The interaction with the shore is therefore ignored, and the problem is assumed to be independent of the channel width.

For the given simplifications the problem will be analyzed by applying the theory for beams on an elastic foundation to a semiinfinite strip of ice of unit width oriented along the channel. Only buoyancy forces will be considered, which means that drag forces and inertia forces acting on the ice when the wave passes are ignored.

In the theory for beams on an elastic foundation the reaction forces from the elastic medium (water in this case) are assumed to be proportional to the deflection of the beam[14]. The proportionality constant is called the modulus of the foundation and will be indicated by k. For water $k=\rho \cdot g (\approx 10^4\ \mathrm{N/m^2})$, where ρ is the density of water and g is the acceleration due to gravity. Let us now assume that the freeboard of the ice sheet, when it is floating on water, is $0.1d$, where d is the thickness of the ice. That means that $0.9d$ of the ice floats below the water surface. Depending on the wave height and the type of wave (positive or negative), one could distinguish different "loading" cases. The buoyancy forces induced by the wave are applied as a distributed load on the ice strip. The distributed load per unit width is indicated by q. As long as a negative wave is lower than $0.9d$ the distributed downward load on the "beam" is proportional to the "local" value of the wave height. For a negative wave higher than $0.9d$ the load does not become larger than $0.9 \cdot d \cdot k$, but the bending moment must be calculated in an iterative way, since the support from the water might "disappear."

The upward load induced by a positive wave cannot be larger than $0.1 \cdot d \cdot k$ if water leakage can occur freely. If the water is higher than $0.1d$ (freeboard of the ice) no further load (buoyancy force) is then imposed by the wave. The different situations that might be encountered regarding the height of the wave compared to the thickness of the ice are summarized in Figure 3.

The case that will be treated in detail in this study is the situation shown in Figure 3a, i.e. a negative wave with a height less than $0.9d$.

Derivation of the bending moments induced by a surge wave

The differential equation for the deflection curve of a beam supported on an elastic foundation is

$$EI \frac{d^4y}{dx^4} = -ky + q \qquad (4)$$

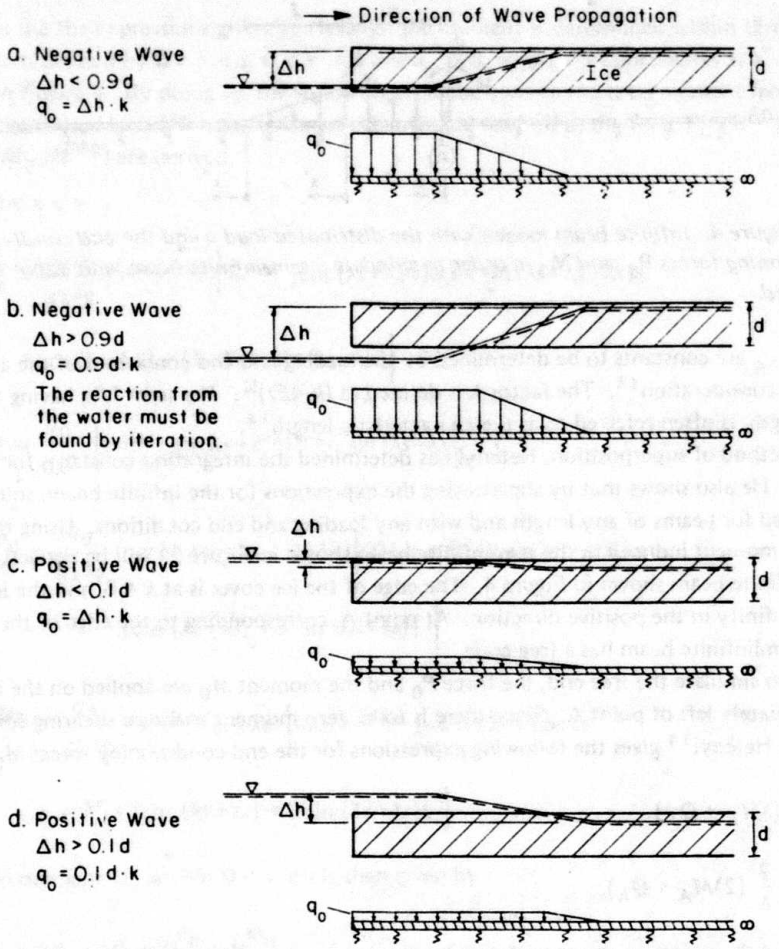

Figure 3. Negative and positive surge waves impinging on the edge of an ice cover. Induced buoyancy forces are applied as a distributed load on a semi-infinite beam simulating a strip of ice along the river.

where EI = flexural rigidity

y = deflection of the beam (positive downward)

x = longitudinal coordinate

k = modulus of the foundation

q = distributed load.[14]

Along the unloaded parts of the beam ($q = 0$) eq 4 will be reduced to

$$EI \frac{d^4y}{dx^4} = -ky. \tag{5}$$

As shown by Hetényi, it is sufficient to consider only the general solution of eq 5, from which solutions can be obtained for cases implied in eq 4 by adding to it a particular integral corresponding to q. The general solution of eq 5 can be written

$$y = e^{\lambda x}(c_1 \cos \lambda x + c_2 \sin \lambda x) + e^{-\lambda x}(c_3 \cos \lambda x + c_4 \sin \lambda x) \tag{6}$$

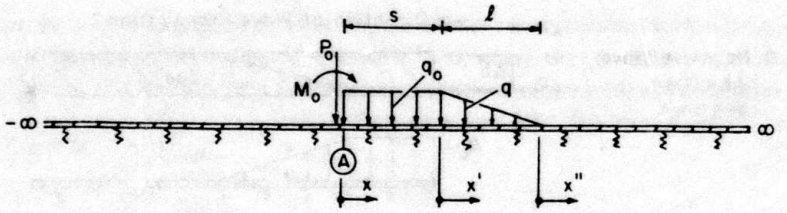

Figure 4. Infinite beam loaded with the distributed load q and the end conditioning forces P_0 and M_0 in order to simulate a semiinfinite beam with a free end.

where c_1 to c_4 are constants to be determined by the loading and end conditions of the actual beam under consideration[14]. The factor λ is defined as $(k/4EI)^{1/4}$. The term $1/\lambda$, having the dimension length, is often referred to as the characteristic length[14].

By the method of superposition, Hetényi has determined the integration constants for an infinite beam. He also shows that by superposing the expressions for the infinite beam, solutions can be derived for beams of any length and with any loading and end conditions. Using this method the bending moment induced in the semiinfinite beam shown in Figure 3a will be derived by analyzing the infinite beam shown in Figure 4. The edge of the ice cover is at $x = 0$, and the ice cover extends to infinity in the positive direction. At point A, corresponding to the edge of the ice cover, the semiinfinite beam has a free end.

In order to simulate the free end, the force P_0 and the moment M_0 are applied on the infinite beam immediately left of point A. Since there is to be zero moment and zero shearing force at the free end, Hetényi[14] gives the following expressions for the end-conditioning forces M_0 and P_0:

$$P_0 = 4(\lambda M_A + Q_A) \tag{7}$$

$$M_0 = -\frac{2}{\lambda}(2\lambda M_A + Q_A) \tag{8}$$

where M_A and Q_A are the moment and shearing force created at point A in the infinite beam by the actual load.

M_A and Q_A are determined by superposing the contributions from the uniformly distributed load on the part of the beam for which $0 < x < s$ and the triangular distributed load for which $0 < x' < \ell$. By inserting the appropriate parameters into the expressions given by Hetényi one finds that:

$$Q_A = \frac{q_0}{4\lambda}\left\{1 - \frac{e^{-\lambda s}}{\lambda \ell} \cdot [e^{-\lambda \ell}\sin(\lambda s+\lambda \ell) - \sin \lambda s]\right\} \tag{9}$$

$$M_A = \frac{q_0}{8\lambda^3 \ell} \cdot e^{-\lambda s}\left\{-e^{-\lambda \ell}[\cos(\lambda s+\lambda \ell) + \sin(\lambda s+\lambda \ell)] + \sin \lambda s + \cos \lambda s\right\}. \tag{10}$$

Substituting eq 9 and 10 into eq 7 and 8, one gets

$$P_0 = \frac{q_0}{2\lambda^2 \ell}\left\{2\lambda \ell + e^{-\lambda s}[3\sin \lambda s + \cos \lambda s - e^{-\lambda \ell}[\cos(\lambda \ell+\lambda s) + 3\sin(\lambda \ell+\lambda s)]]\right\} \tag{11}$$

$$M_0 = \frac{q_0}{2\lambda^3 \ell}\left\{-\lambda \ell + e^{-\lambda s}[-2\sin \lambda s - \cos \lambda s + e^{-\lambda \ell}[\cos(\lambda \ell+\lambda s) + 2\sin(\lambda \ell+\lambda s)]]\right\}. \tag{12}$$

The bending moment in the semiinfinite beam can now be determined by applying the calculated end conditioning forces P_0 and M_0, together with the distributed load on the infinite beam. To

be able to use the expressions given by Hetényi, the moment is determined within three sections of the beam defined by $0 < x < s$, $0 < x' < \ell$ and $x'' > 0$, where the coordinates x, x' and x'' are defined in Figure 4. By doing so, the following contributions to the total moment from the triangular distributed load (M^q), the uniformly distributed load (M^s), the force P_0 (M^{P0}), and the moment M_0 (M^{M0}) are derived.

Within $0 < x < s$

$$M_x^q = \frac{q_0}{8\lambda^3\ell} \cdot e^{-\lambda(s-x)} \left\{ -e^{-\lambda\ell} \left[\cos(\lambda s + \lambda\ell - \lambda x) + \sin(\lambda s + \lambda\ell - \lambda x) \right] \right.$$

$$\left. + \cos(\lambda s - \lambda x) + (1 - 2\lambda\ell) \sin(\lambda s - \lambda x) \right\} \tag{13}$$

$$M_x^s = \frac{q_0}{4\lambda^2} \left\{ e^{-\lambda x} \cdot \sin \lambda x + e^{-\lambda(s-x)} \sin(\lambda s - \lambda x) \right\} \tag{14}$$

$$M_x^{P0} = \frac{q_0}{8\lambda^3\ell} \cdot e^{-\lambda x} (\cos \lambda x - \sin \lambda x) \left\{ 2\lambda\ell + e^{-\lambda s} \left[3 \sin \lambda s + \cos \lambda s \right. \right.$$

$$\left. \left. - e^{-\lambda\ell} \cdot \left[\cos(\lambda\ell + \lambda s) + 3 \sin(\lambda\ell + \lambda s) \right] \right] \right\} \tag{15}$$

$$M_x^{M0} = \frac{q_0}{4\lambda^3\ell} \cdot e^{-\lambda x} \cdot \cos \lambda x \left\{ -\lambda\ell + e^{-\lambda s} \left[-2 \sin \lambda s - \cos \lambda s \right. \right.$$

$$\left. \left. + e^{-\lambda\ell} \cdot \left[\cos(\lambda\ell + \lambda s) + 2 \sin(\lambda\ell + \lambda s) \right] \right] \right\} . \tag{16}$$

The total moment M_x within $0 < x < s$ is then given by

$$M_x = M_x^s + M_x^q + M_x^{P0} + M_x^{M0} . \tag{17}$$

Within $0 < x' < \ell$

$$M_{x'}^q = \frac{q_0}{8\lambda^3\ell} \left\{ -e^{-\lambda(\ell - x')} \left[\cos(\lambda\ell - \lambda x') + \sin(\lambda\ell - \lambda x') \right] \right.$$

$$\left. + e^{-\lambda x'} \cdot \left[\cos \lambda x' + (1 + 2\lambda\ell) \sin \lambda x' \right] \right\} \tag{18}$$

$$M_{x'}^s = \frac{q_0}{4\lambda^2} \cdot e^{-\lambda x'} \left[e^{-\lambda s} \cdot \sin(\lambda x' + \lambda s) - \sin \lambda x' \right] \tag{19}$$

$$M_{x'}^{P0} = \frac{q_0}{8\lambda^3\ell} \cdot e^{-\lambda(x' + s)} \left[\cos(\lambda x' + \lambda s) - \sin(\lambda x' + \lambda s) \right] \left\{ 2\lambda\ell \right.$$

$$\left. + e^{-\lambda s} \cdot \left[3 \sin \lambda s + \cos \lambda s - e^{-\lambda\ell} \left[\cos(\lambda\ell + \lambda s) + 3 \sin(\lambda\ell + \lambda s) \right] \right] \right\} \tag{20}$$

$$M_{x'}^{M0} = \frac{q_0}{4\lambda^3\ell} \cdot e^{-\lambda(x' + s)} \cos(\lambda x' + \lambda s) \left\{ -\lambda\ell + e^{-\lambda s} \left[-2 \sin \lambda s - \cos \lambda s \right. \right.$$

$$\left. \left. + e^{-\lambda\ell} \cdot \left[\cos(\lambda\ell + \lambda s) + 2 \sin(\lambda\ell + \lambda s) \right] \right] \right\} . \tag{21}$$

The total moment $M_{x'}$ within $0 < x' < \ell$ is given by

$$M_{x'} = M^{\ell}_{x'} + M^{s}_{x'} + M^{P_0}_{x'} + M^{M_0}_{x'} . \tag{22}$$

For $x'' > 0$

$$M^{\ell}_{x''} = \frac{q_0}{8\lambda^3 \ell} \cdot e^{-\lambda x''} \left\{ -\cos \lambda x'' - \sin \lambda x'' + e^{-\lambda \ell} \left[\cos (\lambda \ell + \lambda x'') \right.\right.$$

$$\left.\left. + (1 + 2\lambda\ell) \sin (\lambda \ell + \lambda x'') \right] \right\} \tag{23}$$

$$M^{s}_{x''} = \frac{q_0}{4\lambda^2} \cdot e^{-\lambda x''} \left[e^{-\lambda(\ell+s)} \sin (\lambda \ell + \lambda s + \lambda x'') - e^{-\lambda \ell} \sin (\lambda x'' + \lambda \ell) \right] \tag{24}$$

$$M^{P_0}_{x''} = \frac{q_0}{8\lambda^3 \ell} \cdot e^{-\lambda(x''+s+\ell)} \left[\cos (\lambda x'' + \lambda s + \lambda \ell) - \sin (\lambda x'' + \lambda s + \lambda \ell) \right] \left\{ 2\lambda\ell \right.$$

$$\left. + e^{-\lambda s} \left[3 \sin \lambda s + \cos \lambda s - e^{-\lambda \ell} \left[\cos (\lambda \ell + \lambda s) + 3 \sin (\lambda \ell + \lambda s) \right] \right] \right\} \tag{25}$$

$$M^{M_0}_{x''} = \frac{q_0}{4\lambda^3 \ell} \cdot e^{-\lambda(x''+s+\ell)} \cdot \left[\cos (\lambda x'' + \lambda s + \lambda \ell) \right] \left\{ -\lambda\ell + e^{-\lambda s} \left[-2 \sin \lambda s - \cos \lambda s \right.\right.$$

$$\left.\left. + e^{-\lambda \ell} \left[\cos (\lambda \ell + \lambda s) + 2 \sin (\lambda \ell + \lambda s) \right] \right] \right\} . \tag{26}$$

The total moment $M_{x''}$ for $x'' > 0$ is given by

$$M_{x''} = M^{\ell}_{x''} + M^{s}_{x''} + M^{P_0}_{x''} + M^{M_0}_{x''} . \tag{27}$$

Determination of the wave characteristics for which the ice cover breaks

Let us take as an example a triangular wave with a slope of 0.01. (This could correspond to a wave 0.5 m high and 50 m long; see *Stating the problem*, p. 1.) In Table 1, values of λ and $\lambda\ell$ are given for such a wave for different ice thicknesses, assuming that the wave has progressed into the ice cover so that the drop in water level at the edge is equal to $0.9d$.

Table 1. Values of λ, ℓ and $\lambda\ell$ for different ice thicknesses, assuming $E = 6 \cdot 10^9$ N/m² and considering a triangular wave with a slope of 0.01.

Ice thickness (m)	λ (m^{-1})	ℓ (m)	$\lambda\ell$ (m/m)
0.1	0.264	9	2.4
0.2	0.157	18	2.8
0.3	0.116	27	3.1
0.4	0.094	36	3.4
0.5	0.079	45	3.6

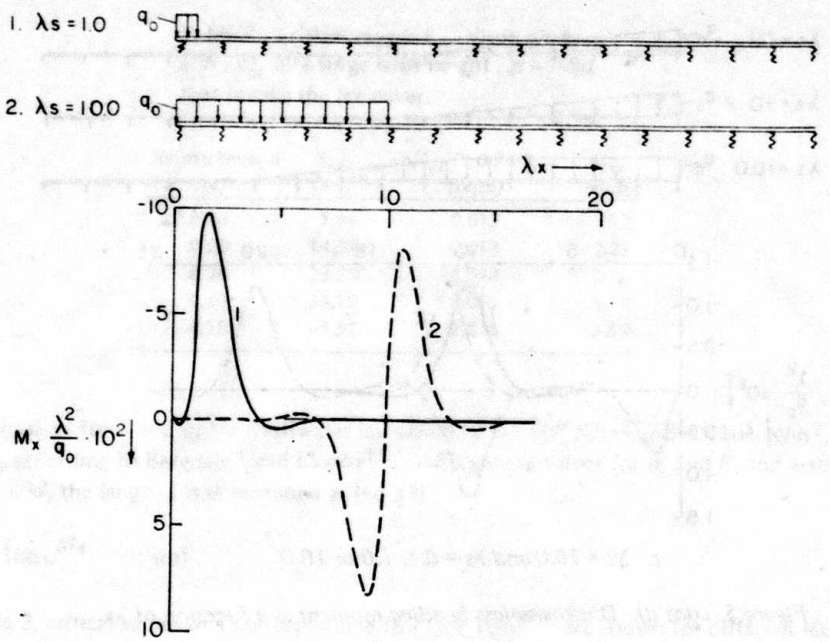

a. $\lambda\ell = 10^{-6}$ and $\lambda s = 1.0$ or 10.0.

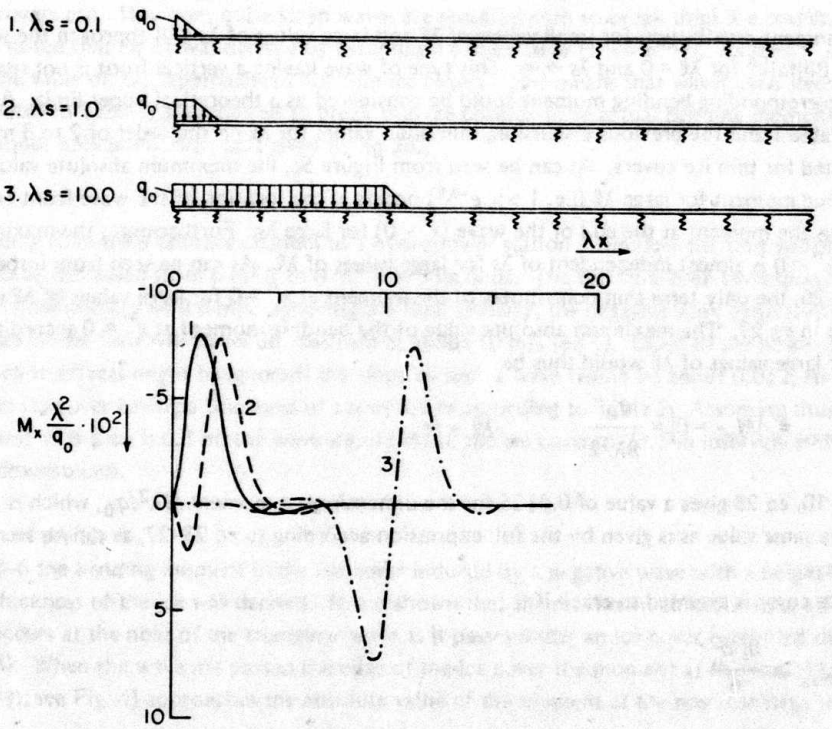

b. $\lambda\ell = 1.0$ and $\lambda s = 0.1$, 1.0 or 10.0.

Figure 5. Dimensionless bending moment as a function of λx.

In Figure 5 the distribution of the bending moment in dimensionless form ($M\lambda^2/q_0$) is shown graphically for $\lambda\ell = 10^{-6}$, $\lambda\ell = 1$ and $\lambda\ell = 10$ according to eq 17, 22 and 27. For each value of $\lambda\ell$, curves for different values of λs are shown.

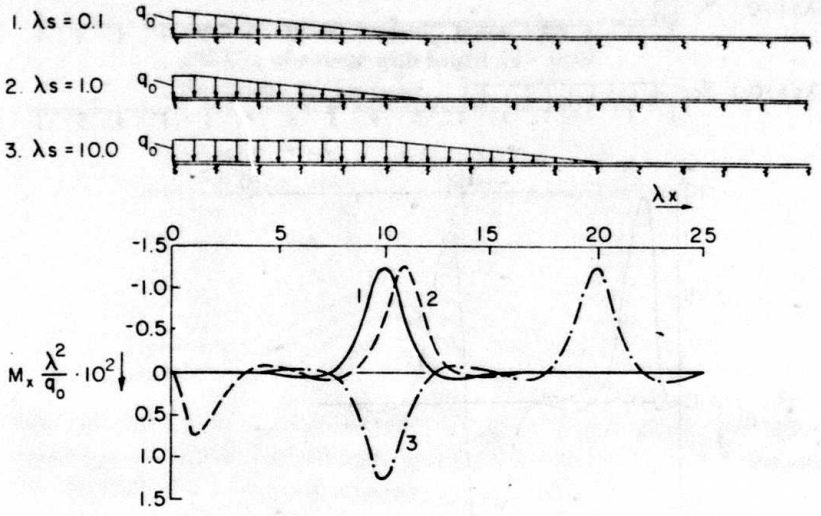

c. λℓ = 10.0 and λs = 0.1, 1.0 or 10.0.

Figure 5 (cont'd). Dimensionless bending moment as a function of λx.

The moment distribution for small values of λℓ and large values of λs will approach the solution given by Billfalk[6] for λℓ = 0 and λs → ∞. This type of wave having a vertical front is not realistic, and the corresponding bending moment could be considered as a theoretical upper limit. As can be seen in Table 1 and the previous discussion, minimum values for λℓ on the order of 2 to 3 might be expected for thin ice covers. As can be seen from Figure 5c, the maximum absolute value of the bending moment for large λℓ (i.e. $1 >> e^{-\lambda\ell}$) occurs at the location of the wave front ($x'' = 0$) and equals the moment at the end of the wave ($x' = 0$) for large λs. Furthermore, the maximum value at $x'' = 0$ is almost independent of λs for large values of λℓ. As can be seen from inspection of eq 23-26, the only term that contributes to the moment at $x'' = 0$ for large values of λℓ is the first term in eq 23. The maximum absolute value of the bending moment at $x'' = 0$ according to eq 27 for large values of λℓ would thus be

$$M_{max} = \left|M_{x''=0}\right| = \frac{q_0}{8\lambda^3\ell} \qquad \lambda\ell \to \infty . \tag{28}$$

For λℓ = 10, eq 28 gives a value of 0.0125 for the dimensionless moment $M\lambda^2/q_0$, which is practically the same value as is given by the full expression according to eq 23-27, as can be seen from Figure 5c.

The ice cover is assumed to crack if

$$M_{max} \geq \frac{\sigma_f d^2}{6} \tag{29}$$

where σ_f = flexural strength of the ice and d = thickness of the ice.

Equations 28 and 29 indicate that the ice breaks if

$$\ell \leq 3.28 \cdot \frac{E^{3/4}}{\sigma_f} \cdot d^{1/4} \cdot \Delta h \tag{30}$$

where the wave height Δh is assumed to be less than $0.9d$ and the modulus of the foundation is set to 10^4 N/m^2 (water).

Table 2. Critical length ℓ_{cr}, slope $\Delta h/\ell_{cr}$ and $\lambda\ell_{cr}$ of a surge with height $\Delta h = 0.9d$ that breaks the ice cover.

Ice thickness d (m)	ℓ_{cr} *(m)*	$\Delta h/\ell_{cr}$ $(= 0.9d/\ell_{cr})$ *(m/m)*	$\lambda\ell_{cr}$ *(m/m)*
0.10	5.96	0.015	1.57
0.20	14.18	0.013	2.23
0.30	23.53	0.012	2.73
0.40	33.72	0.011	3.17
0.50	44.57	0.010	3.52

Typical values for E and σ_f for freshwater ice would be $6 \cdot 10^9$ N/m^2 and $6 \cdot 10^5$ N/m^2, respectively, according to Bergdahl[4] and Lavrov[15]. Taking these values for σ_f and E, and assuming that $\Delta h = 0.9d$, the length ℓ is determined as (eq 30)

$$\ell < 106 d^{5/4} \quad \text{(m)} . \tag{31}$$

In Table 2, critical values of ℓ corresponding to $\ell_{cr} = 106d^{5/4}$ are shown for different ice thicknesses. The critical slopes of the wave front defined as $\Delta h/\ell_{cr}$ (for $\Delta h = 0.9d$) are also shown.

As can be seen from Table 2, thin ice covers can resist steeper waves without breaking than thick ice covers can. However, quite steep waves are required even to break thick ice covers. It should be noted that eq 31 was derived by assuming $\lambda\ell$ to be large ($1 >> e^{-\lambda\ell}$). As seen from Table 2, the value of $\lambda\ell_{cr}$ approaches 1 for thin ice covers. This means that waves even steeper than indicated in Table 2 are required to break thin ice covers. (The actual bending moment for $\lambda\ell = 1$ is about 35% lower than that given by eq 28.)

Example

Consider a 10-m-deep tail-race channel to a hydropower station. The flow per unit width is assumed to be decreased from 6 m^2/s to 0 m^2/s in 5 seconds. The full flow then corresponds to an average flow velocity of 0.6 m/s. Ignoring the flow velocity, the negative wave generated by the decrease of the flow will travel downstream at about 10 m/s (eq 1). Close to the power station (where friction effects might be ignored) the slope of such a wave would be about 0.012, enough to break an ice cover having a thickness of about 0.3 m according to Table 2. Assuming thus that the thickness of the ice is 0.3 m, the wave should break the ice cover at 23.5-m intervals as it advances downstream.

Deflection of the ice

On p. 3–6 the bending moment in the ice cover induced by a negative wave with a height less than the thickness of the ice was derived. It was shown that the maximum absolute value of the moment occurs at the nose of the triangular wave as it passes under an ice cover (provided that $1 >> e^{-\lambda\ell}$). When the wave has passed the edge of the ice cover the moment at the end of the wave ($x' = 0$; see Fig. 4) approaches the absolute value of the moment at the nose for large values of λs.

Let us now analyze the deflection for the case when $s = 0$ (see Fig. 4). The deflection around the nose of the wave, for large values of $\lambda\ell$ ($1 >> e^{-\lambda\ell}$), will be almost the same as for the case $s > 0$. Using the solutions given by Hetényi for an infinite beam, the deflection of the semiinfinite strip of ice is found by applying the triangular distributed load and the conditioning forces P_0 and M_0 on the infinite beam. Ignoring terms that are small for large values of $\lambda\ell$ (e.g. $1 >> e^{-\lambda\ell}$) the deflection within the wave ($0 < x' < \ell$) and to the right of the wave nose ($x'' > 0$) can be well approximated by the following expressions ($\lambda s = 0$ at $x = x'$):

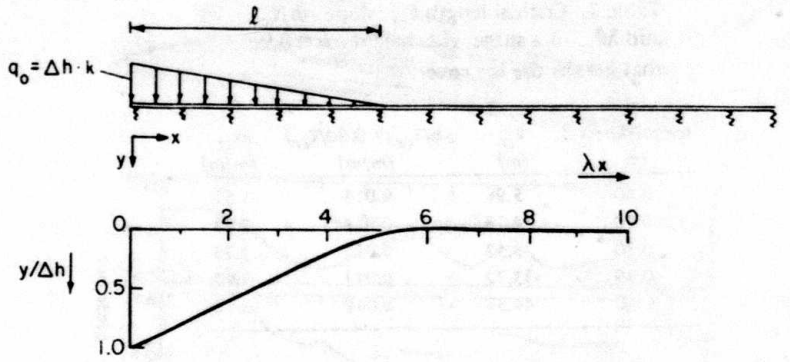

Figure 6. Deflection of the edge of the ice cover for the wave height $\Delta h \leq 0.9d$, $\lambda\ell = 5$ and $s = 0$ according to eq 32 and 33.

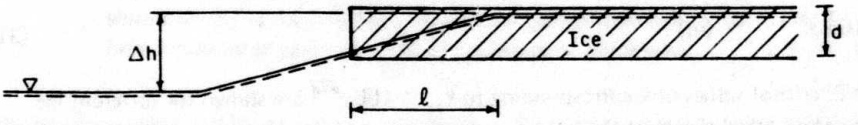

Figure 7. Wave height larger than the thickness of the ice.

$$\frac{y}{\Delta h} = \frac{\ell - x}{\ell} + \frac{e^{-\lambda(\ell - x)}}{4\lambda\ell}\left[\cos(\lambda\ell - \lambda x) - \sin(\lambda\ell - \lambda x)\right] \qquad \text{for } \lambda s = 0 \text{ and } 0 < x < \ell \qquad (32)$$

$$\frac{y}{\Delta h} = \frac{e^{-\lambda(\ell - x)}}{4\lambda\ell}\left[\cos(\lambda x - \lambda\ell) - \sin(\lambda x - \lambda\ell)\right] \qquad \text{for } \lambda s = 0 \text{ and } x > \ell\ . \qquad (33)$$

These expressions are shown graphically in Figure 6 for $\lambda\ell = 5$. As can be seen, most of the bending takes place at the nose of the wave; very little occurs along the rest of the wave front.

Consider now the case shown in Figure 7, where the wave height Δh is larger than $0.9d$. As long as the wave front is not steeper than $0.9d$, $\lambda\ell$ can be considered large ($1 >> e^{-\lambda\ell}$). This case can be treated in an approximate way by calculating the deflection (and the moment) for the nose and the end of the wave separately, assuming that negligible bending takes place along the central part of the wave.

DISCUSSION AND FIELD OBSERVATIONS

The bending moment induced in an ice cover by the passage of a negative wave with linearly sloping front has been derived for waves lower than $0.9d$. The derived moment distribution is, in principle, also valid for a positive wave just by changing the sign of the moment.

In the present study the ice cover is assumed to float freely from the shores. The maximum distributed load q_0 induced by a positive wave is therefore assumed to be about $0.1 \cdot d \cdot k$ (see Fig. 3). Let us now consider a very steep positive wave, and try to estimate if such a wave could break an ice cover under this assumption. As can be seen from Figure 5, the maximum bending moment for $\lambda\ell = 10^{-6}$ (practically vertical front) will be on the order of $0.1 \cdot q_0/\lambda^2$. With $q_0 = 0.1 \cdot d \cdot k$ the resulting moment will give rise to a bending stress in the ice cover of about 10^5 N/m^2, which is less than the typical bending strength of freshwater ice. This indicates that under the given assumptions

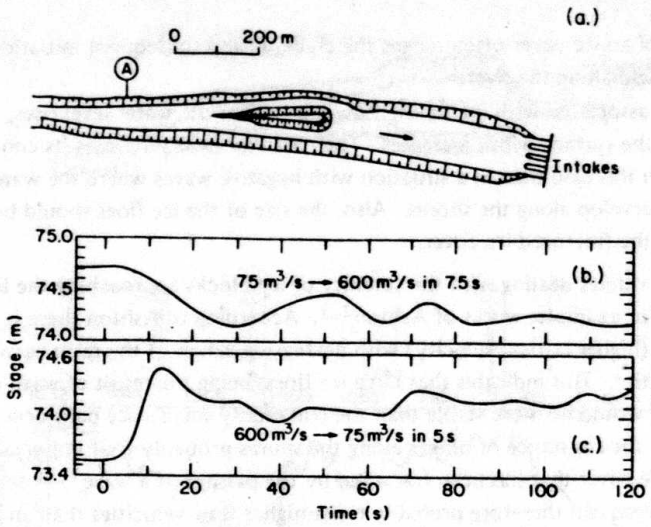

Figure 8. Water level variations at load acceptance (b) and at shutdown (c) in the headrace channel of Stornorrfors power station measured at point A, 1000 m upstream of the intake.

the buoyancy forces induced by a positive wave should not be able to break a freely floating ice cover unless the ice is weakened (as it usually is at spring breakup).

If the ice cover is frozen to the shores, or the leakage of water through the cracks along the shores is small, a positive wave presumably could induce a distributed load which is larger than $0.1 \cdot d \cdot k$ and thereby be able to break the ice cover.

To check the validity of the presented theory, laboratory experiments or well-controlled field tests should be done. In order to provide some insight into the characteristics of waves generated by rapid discharge variations some field observations from Swedish power stations will be discussed. Furthermore, some field measurements of water level variations associated with the formation and breakup of ice jams will be briefly discussed.

For the theoretical analysis a surge wave with linearly sloping front has been assumed. Such an "ideal wave" can be approximated in a uniform channel by a constant rate of change of the flow. Waves generated by discharge variations in hydroelectric power stations may, however, depart from the assumed "ideal form" for many reasons. For example, the typical rate of flow variation is not perfectly linear. Furthermore, the waterways often have a nonuniform geometry.

Water level variations have been measured at a point located 1000 m upstream of Stornorrfors power station in Sweden (point A, Fig. 8a) during tests with rapid discharge variations under ice-free conditions. The surface width is about 65 m at point A and increases to about 140 m at the intake. From a steady flow of 75 m^3/s the total flow through the three turbines was increased to 600 m^3/s at load acceptance by opening the wicket gates in 7 to 8 seconds. The resulting water level variation at point A is shown in Figure 8b. At load rejection the flow was decreased from 600 m^3/s to 75 m^3/s by closing the wicket gates in about 5 seconds. The measured water level variation at point A in this case is shown in Figure 8c.

Considering the actual water depth, the wave speed and the wave form along the headrace channel can be estimated from the stage measurements shown in Figure 8. The average slopes of the negative and positive wave fronts were thus found to be about 0.003 and 0.018. The negative wave, assuming normal ice strength, would not be steep enough to break a solid ice cover. The positive wave was much steeper but, as already discussed, positive waves should not be able to break an ice cover unless the ice is frozen to the shore.

At this point it should perhaps be noted that only the occurrence of cracks in the ice cover, due to the passage of a wave, can be predicted by the theory presented. Sometimes in the text this process has been referred to as breakup of the ice cover. This is an important distinction,

since the breakup of an ice cover often means the cracking and subsequent initiation of movement of the broken ice field along the river.

A positive wave associated with increasing flow means that the water level rises, and for most natural waterways the surface width increases. The ice cover probably loses its contact with the shore more easily in this case than in a situation with negative waves where the water level decreases and hinges develop along the shores. Also, the size of the ice floes should be of importance for the stability of the fractured ice cover.

There are many studies dealing with the stability of ice blocks approaching the leading edge of an ice cover. See, for example, works of Ashton[2,3]. According to Ashton there is a weak trend of increasing stability (higher critical velocity) with decreasing values of the ratio between ice thickness and block length[3]. This indicates that large ice floes, being the result of wave-induced breakup of a solid ice cover, would be more stable than the commonly smaller ice pans occurring at freeze-up of a river. Also, the resistance of hinges along the shores probably is of importance for the overall stability of an ice cover that has been fractured by the passage of a wave[1]. A solid ice cover that has been fractured can therefore probably resist higher flow velocities than an unconsolidated ice cover formed during freeze-up.

Let us now discuss a test of the stability of a solid ice cover on the headrace channel of Malfors power station in southern Sweden. During a shutdown over a cold weekend, 10–11 February 1976, a 7-cm-thick ice cover was formed over the 1600-m-long headrace channel. Close to the intake the channel has been widened to form a 100-m-long forebay before the water enters a narrow, 120-m-long concrete flume leading to the penstock (see Fig. 9a).

The purpose of the test was to investigate the stability of a solid ice cover during rapid flow variations. During the test the water level was measured at three locations in and near the forebay by submerged pressure gauges (Fig. 9a, locations 1, 2 and 3). On the morning of 12 February the flow was increased from 0 m^3/s to 60 m^3/s in 15 minutes, kept constant for about 5 minutes, and then decreased to 0 m^3/s in another 15 minutes. During this slow variation of the flow the ice cover broke along the shores of the channel, but apart from shore cracks the ice cover remained intact. After this slow variation very rapid discharge variations were tested at successively higher maximum flows, as summarized below:

Test	*Discharge (m^3/s)*
1	0 → 10 → 0
2	0 → 20 → 0
3	0 → 40 → 0
4	0 → 60 → 0
5	0 → 84 (max)

During the first four tests the ice cover remained stable (observations were made only from the downstream end of the forebay). A couple of minutes after the flow had reached its maximum in the 5th test the ice cover collapsed on the channel just upstream of the forebay.

The water level variation at point 3, that is, about 60 m upstream of the forebay, is shown for tests 4 and 5 in Figure 9b. As can be seen, steady state was not reached, either at maximum or at zero flow.

The average slope of the water level over a "longer" period of time was hardly steep enough to cause the fracturing of the ice cover that presumably preceded the collapse in test 5. However, very rapid stage variations superposed on the slower water level variations did appear. See, for example, the steep rise in water level at 1050 and the sudden drop at about 1053 in Figure 9b. The theory presented is not valid for the irregular wave form shown in Figure 9b. It is estimated, however, based on the theory, that the sudden drop in water level at about 1053 was steep enough to fracture the ice.

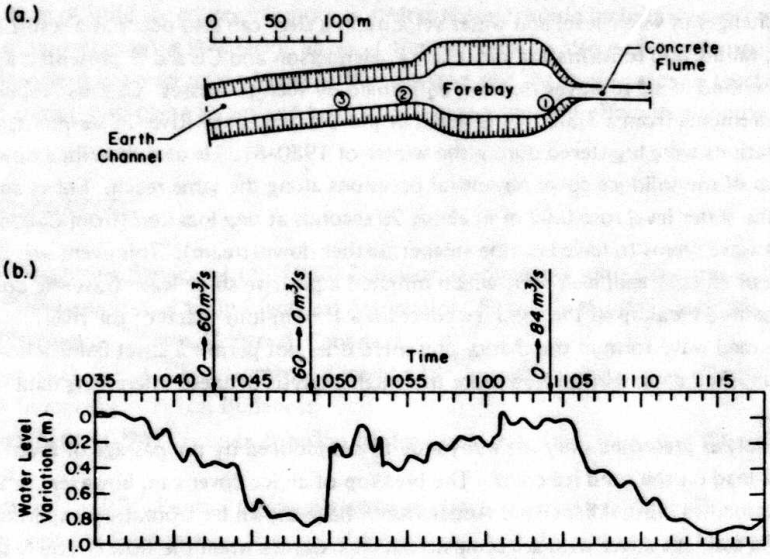

Figure 9. Water level variations at point 3 in the headrace channel of Malfors power station.

The collapse of the ice cover that occurred at about 1107 was apparently initiated at the exit of the channel in the forebay. Suddenly, ice floes seemed to be rotated over the entire width of the channel at this section. The ice cover on the channel then started to move downstream and slid under the ice cover on the forebay. Although the ice cover on the forebay developed some cracks it remained stable. The moving ice cover on the channel had been broken into floes of different sizes. About 10 minutes after the maximum discharge was reached the power plant had to be shut down because the broken ice blocked the trash racks at the intake.

Let us try to estimate the in-plane force required to make the broken ice field, resting against the solid ice cover on the forebay, unstable. It can be shown that the in-plane force per unit width, F_{cr}, needed to cause incipient instability of a broken ice field is

$$F_{cr} = {}^{1}/_{12}\ \rho g L^2 \tag{34}$$

where L is the length of the ice floe along the channel[19]. In an ice cover that is forming by accumulation of ice floes the pressure at a given section increases with increasing distance to the leading edge. This holds as long as the distance to the edge is less than about three to six times the river width. Additional forces due to accumulation of more ice at the edge are transmitted to the shores, and the pressure at the considered section levels off[16]. In a solid ice cover that has been fractured the pressure at a given section might be assumed to increase even for longer distances to the edge than in the case of a fractured ice cover built up of drifting ice floes

No close observations were made at the location where the collapse of the ice cover was initiated. The size of the floes that formed when the solid ice was first fractured at this section is therefore not well known. From pictures taken somewhat later of the moving ice on the channel it is estimated that the smaller floes were on the order of 1 m long. The force required to create instability of such ice floes is about 820 N/m according to eq 34. It seems reasonable that such a force could be induced by the flow (unsteady) in the channel, since the contact between the ice cover and the shore probably was weak due to well developed shore cracks. Thus the collapse of the solid ice cover in this case seems to be explicable as being the result of the passage of a steep wave and the instability mechanism described by eq 34.

Rapid changes in water level and water velocity in a river can also occur as a result of the sudden formation, failure and re-formation of ice jams. Henderson and Gerard[13] presented a theoretical study of the kind of surge waves that can be formed by such processes. Calkins[7] reported some field measurements from a 3.3-km-long reach of the Ottauquechee River in Vermont, where such surge formations were registered during the winter of 1980–81. He also described observations of the breakup of the solid ice cover on several occasions along the same reach. For example, on 11 February the water level rose 0.62 m in about 20 seconds at one location (from Calkins' published figures this wave seems to have become steeper further downstream). This event was the result of breakup of an upstream ice cover, which initiated a positive surge wave traveling downstream. The wave caused breakup of the solid ice cover on a 1.3-km-long reach of the river.

The assumed wave form in the theory presented does not permit a strict comparison with Calkins' published data. However, a more thorough analysis of these interesting data should be performed.

In the analysis presented only the buoyancy forces induced by the passage of a wave are considered as a load on the solid ice cover. The breakup of an ice cover can, however, be induced by high flow velocities only. Michel and Abdelnour[17] have shown by laboratory experiment how the breakup of a solid ice cover with a free upstream edge occurs when the flow is slowly increased. Even though their analysis is questionable, the experiments show that no waves are required to cause breakup of a solid ice cover[6].

Downstream from a power station a rapid increase of the discharge causes a positive wave and increased flow velocity. If the flow velocity is high, the flow-induced forces may have the same ability to break the ice cover as the buoyancy forces induced by a wave. Consequently the breakup of a solid ice cover can be caused by waves smaller or less steep than those assumed in the theory presented.

SUMMARY

The purpose of this study was to analyze under what circumstances rapid water level fluctuations can cause breakup of a solid river ice cover. The analysis is restricted to considering the buoyancy forces induced in the ice cover when a surge wave with a linearly sloping front passes the edge of the ice cover (see Fig. 2 and 3). This means that the action of the wave is considered as a static load by "freezing" the wave at different locations along the ice cover (Fig. 4). Furthermore, the interaction with the shore is ignored, and the problem is assumed to be independent of the river width.

For the given simplifications the problem is analyzed by applying the theory for beams on an elastic foundation to a semiinfinite strip of ice oriented along the river. Using the method of superposition, and solutions given by Hetényi[14] for an infinite beam, the bending moment induced in the semiinfinite strip of ice shown in Figure 3a has been derived. Bending moment distributions for different steepness and location of the wave front are shown in Figure 5. Where the induced bending moment exceeds the flexural strength of the ice a crack is assumed to occur.

One of the conclusions of the study is that thin ice covers can resist steeper waves without breaking than thick ice covers can. However, quite steep waves are required to break even thick ice covers.

Most common rates of discharge variation at hydropower stations will not generate steep enough waves to break a solid ice cover on adjacent waterways. Very rapid flow variations occurring, for example, at shutdowns or very rapid load acceptances could, however, cause fracturing of a solid ice cover.

Very steep waves can be generated by the collapse of ice jams as can be seen from field measurements in the Ottauquechee river[7]. The measured waves show a form that differs from the triangular form adopted for the theory presented here. A strict comparison between the observations and the theory is therefore not possible. However, a more thorough analysis of these data is needed.

The present theory should be considered as a first estimation of the significance of surge waves in the breakup of solid ice covers. A more complete theory should include dynamic effects, which might be of importance for very steep waves. Other wave forms also ought to be analyzed, and the significance of the interaction between the ice cover and the shore needs to be clarified. The combined action of in-plane forces and buoyancy forces is another effect that should be analyzed.

LITERATURE CITED

1. **Acres Consulting Services, Ltd.** (1980) Behavior of ice covers subject to large daily flow and level fluctuations. Canadian Electrical Association, Research and Development, Suite 580, One Westmount Square, Montreal, Canada.
2. **Ashton, G.D.** (1974a) Entrainment of ice blocks: Secondary influences. Proceedings IAHR Symposium on Ice, Budapest.
3. **Ashton, G.D.** (1974b) Froude criterion for ice-block stability. Journal of Glaciology, vol. 13, no. 68.
4. **Bergdahl, L.** (1977) Physics of ice and snow as affects thermal pressure. Chalmers University of Technology, Gothenburg, Sweden, Report Series A: 1, Department of Hydraulics.
5. **Billfalk, L.** (1981) Formation of shore cracks in ice covers due to changes in the water level. Proceedings IAHR Symposium on Ice, Quebec, Canada.
6. **Billfalk, L.** (1981) Ice cover formation on rivers: Effects of short-time flow regulation. Bulletin 106, Hydraulics Laboratory, Royal Institute of Technology, Stockholm, Sweden (in Swedish with English summary).
7. **Calkins, D.J.** (1981) Field measurements of the hydraulic transients during the ice cover formation and break-up: Ottauquechee River 1980–81. USA Cold Regions Research and Engineering Laboratory, Technical Note (unpublished).
8. **Carter, D., Y.Ouellet and P. Pay** (1981) Fracture of a solid ice cover by wind-induced or ship-generated waves. Proceedings 6th Conference on Port and Ocean Engineering Under Arctic Conditions, Quebec, Canada, vol. II, p. 843–856.
9. **Donchenko, R.V.** (1975) Conditions for ice jam formation in tailwaters. Gosudarstvennyi Gidrologicheskii Institute, Leningrad, Trudy, vol. 227, p. 31–45. Draft Translation 669, USA Cold Regions Research and Engineering Laboratory, 1978.
10. Flow fluctuation tests Winnipeg River Redevelopment, Hydrology Report No. 2, System Planning Division, Hydro Dev. Dept. Report No. 76-20, 760521.
11. **Foulds, D.M.** (1981) Peaking hydro generating stations in winter. Proceedings IAHR Symposium on Ice, Quebec, Canada.
12. **Henderson, F.M.** (1966) Open channel flow. New York: MacMillan.
13. **Henderson, F.M. and R. Gerard** (1981) Flood waves caused by ice jam formation and failure. Proceedings IAHR Symposium on Ice, Quebec, Canada.
14. **Hetényi, M.** (1946) Beams on elastic foundation. Ann Arbor: The University of Michigan Press.
15. **Lavrov, V.V.** (1969) Deformation and strength of ice. Gidrometeorologicheskoe Izdatel'stvo, Leningrad. Translation by Israel Program for Scientific Translations, Jerusalem, 1971.
16. **Michel, B.** (1968) Thrust exerted by an unconsolidated ice cover on a boom. National Research Council of Canada, Technical Memorandum 92, p. 163–170. Associate Committee on Geotechnical Research, Ottawa.
17. **Michel, B. and R. Abdelnour** (1975) Break-up of a solid ice cover. Proceedings of IAHR Symposium on Ice, Hanover, New Hampshire.
18. **Sjöberg, A.** (1976) Calculation of unsteady flow in regulated rivers and storm sewer systems. Chalmers University of Technology, Gothenburg, Sweden, Report No. 87, Department of Hydraulics.
19. **Sodhi, D. and L. Billfalk** (in prep.) Instability of a broken ice cover caused by combined frictional drag and wave action. USA Cold Regions Research and Engineering Laboratory.

A facsimile catalog card in Library of Congress MARC format is reproduced below.

Billfalk, Lennart
Breakup of solid ice covers due to rapid water level variations / by Lennart Billfalk. Hanover, N.H.: U.S. Cold Regions Research and Engineering Laboratory; Springfield, Va.: available from National Technical Information Services, 1982.
iv, 24 p., illus.; 28 cm. (CRREL Report 82-3.)
Prepared for Office of the Chief of Engineers by Swedish State Power Board.
Bibliography: p. 17.
1. Ice. 2. Ice breakup. 3. Ice formation. 4. Rivers. I. United States. Army. Corps of Engineers. II. Army Cold Regions Research and Engineering Laboratory, Hanover, N.H. III. Series: CRREL Report 82-3.